

Measurement of Density-Sensitive Electric Quadrupole Transitions in Neonlike Laser-Produced Plasmas

B. K. F. Young, A. L. Osterheld, R. S. Walling, W. H. Goldstein, T. W. Phillips, and R. E. Stewart
Lawrence Livermore National Laboratory, University of California, Livermore, California 94550

G. Charatis and Gar. E. Busch
KMS Fusion, Inc., Ann Arbor, Michigan 48106
(Received 26 September 1988)

We report on the measurement of density-sensitive electric quadrupole transitions in neonlike molybdenum and silver laser-produced plasmas. These observations are unique in that they represent data which are simultaneously space and time resolved. The electron densities were determined using holographic interferometry. We test the predicted density sensitivity of the electric quadrupole transitions and find excellent agreement with calculations using a detailed, steady-state, collisional-radiative model of the neonlike charge state.

PACS numbers: 32.70.Fw, 42.40.My, 52.25.Nr, 52.40.Nk

The characterization of hot dense plasmas has become especially important due to recent studies of short-wavelength lasing schemes based on high-powered, laser-produced neonlike plasmas.¹ This has spawned a flurry of activity to measure and model the complex *L*-shell (fluorinelike, neonlike, sodiumlike, etc.) x-ray emissions.²⁻⁶ In this Letter, we focus on the measurement of an electric quadrupole (*E2*) transition, “*x*” [$2s^2p^6-3d(\frac{1}{2}, \frac{5}{2}), J=2$ to $2s^2p^6(0,0), J=0$], in Ne-like Mo³²⁺ and Ag³⁷⁺. These transitions have been observed in time-integrated spectra from laser-produced plasmas by Gauthier and co-workers^{7,8} for a range of elements from strontium ($Z=38$) to silver ($Z=47$) and in molybdenum by Phillips and MacGowan.⁹ These *E2* lines have also been observed in low-density tokamak plasmas.^{10,11} The *E2* transitions are predicted to be sensitive to the electron density, using steady-state, collisional-radiative model calculations which are briefly described in this Letter. We test the density dependence of the *E2* transitions by comparing experimental to theoretical line-intensity ratios as a function of the measured electron density.

The application of x-ray emission features to characterize the local plasma conditions is difficult due to the highly transient nature of these laser-produced plasmas. In the experiments reported here, we have minimized these effects by using spectra which are simultaneously space and time resolved. The data presented in this report were a part of a series of microdot x-ray spectroscopy experiments performed using the CHROMA laser at KMS Fusion, Inc. A more detailed discussion of these experiments can be found in Refs. 12-14. The targets consisted of microdots of either pure silver or a mixture of molybdenum and magnesium (Mo:Mg=1:8) mounted on thick plastic substrates.¹⁵ The diluted Mo-Mg target greatly reduced line opacity effects. The microdots were heated by a 0.53- μm , 1.0-ns-wide stacked pulse (tra-

pezoidal shape with a 100-ps rise and fall time and a 1.0-ns flat top) to intensities of 4.1×10^{14} (Ag) and 3.2×10^{14} W/cm² (Mo-Mg).

The simultaneously space- and time-resolved emission spectra were measured by a framing crystal x-ray spectrometer (FCXS) aligned to view the target nearly perpendicular to the laser axis.^{13,14} A common timing fiducial provided time accuracies of 5 ps with respect to the start of the CHROMA heating pulse. A set of framed Mo-Mg spectra for this experiment is shown in Fig. 1. Each image represents the recorded spectra versus the spatial extent of the plasma emission over a 250-ps time interval. A set of 50- μm -wide imaging slits were used. The molybdenum *L*-shell spectra between 3.7 and 5.4 Å

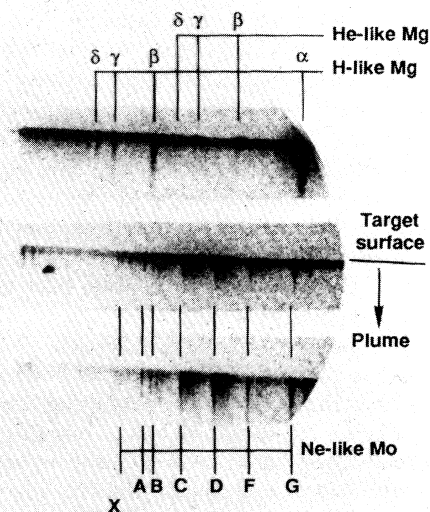


FIG. 1. A set of framed, space-resolved spectra for a Mo-Mg target measured with the FCXS: Mg *K*-shell spectra for 230-480 ps (top), and Mo *L*-shell spectra for 230-480 ps (middle) and 730-980 ps (bottom).

were measured with a beryl crystal at 230–480 ps (middle strip) and 730–980 ps (bottom strip) from the start of the CHROMA heating pulse. The top image shows magnesium *K*-shell spectra measured at 230–480 ps using a potassium acid phosphate (KAP) crystal.

Molybdenum and silver spectra emitted from a 50- μm region of plasma centered at 70 μm from the target surface are shown in Figs. 2(a) and 2(b). These spectra were obtained from densitometer scans of the 230–480-ps FCXS time frames. All intensities have been corrected for the film response, crystal reflectivities, filter transmissions, and photocathode efficiencies.^{13,14} Spatial line-intensity profiles for various spectral features were determined from a series of similar densitometer scans for each time interval. Simultaneous, nonspectroscopic measurements of electron density profiles were obtained from a four-frame holographic interferometer.¹⁶

The electron temperature was estimated using the magnesium *K*-shell spectra recorded simultaneously by

the FCXS at 230–480 ps. Ratios of hydrogenlike to heliumlike resonance line intensities were compared with those predicted by the steady-state, collisional-radiative equilibrium model RATION¹⁷ to infer the electron temperature profile. Because the plasma is overionized, the temperatures obtained by this method overestimate the actual electron temperatures.¹² We find the temperature profile increases away from the target surface: about 350 eV at 24 μm to 850 eV at 212 μm from the target surface for this time interval. The x-ray transitions used for this analysis are not strongly temperature dependent.

We have predicted the density dependence of the Ne-like emission using a steady-state, collisional-radiative neonlike model for the population kinetics of the $2s^2 2p^6$ ground state and 88 excited levels contained in the $2s^2 2p^5 3l$, $2s 2p^6 3l$, $2s^2 2p^5 4l$, and $2s 2p^6 4l$ configurations.⁴ The model included all *E1*, *E2*, and important *M1* and *M2* radiative decays, and all electron-impact transitions. Energy levels and radiative decay rates were computed in the relativistic, parametric central potential model.^{18,19} Multiconfigurational, distorted-wave collisional rate coefficients were calculated using methods recently developed by Bar-Shalom, Klapisch, and Oreg.²⁰

The *x* excited level is strongly populated in these dense, laser-produced plasmas by the large *E2* electron-collisional excitation rate from the $2s^2 2p^6$ ground state.²¹ However, the *E2* radiative decay rate of this level is difficult to observe owing to competing collisional depopulation rates. In high-*Z* plasmas ($Z \geq 37$), the *E2* x-ray transitions can be seen up to densities near 10^{21} cm^{-3} because of the *Z* scaling of the *E2* rates (approximately Z^6 , versus Z^4 for *E1* transitions). This allows us to infer the population kinetics of these metastable levels. We have investigated the density dependence of the ratio of the electric quadrupole *x* and electric dipole *3A* [$2s 2p^6 3p(\frac{1}{2}, \frac{1}{2}), J=1$ to $2s^2 2p^6, J=0$] decays. At low densities, collisional transitions between excited states are not important and the *x/3A* line-intensity ratio is independent of density. At electron densities above 10^{18} cm^{-3} , the population of the *3A* level is increasingly enhanced by collisional transitions from nearby metastable levels, in particular, the [$2s 2p^6 3s(\frac{1}{2}, \frac{1}{2}), J=0$] level. Above $2 \times 10^{20} \text{ cm}^{-3}$ collisional depopulation gradually reduces the strength of the *x* transition. The densities quoted are for the Mo^{32+} ions; similar results apply to the Ag^{37+} ions. Thus, the *x/3A* line ratio decreases with electron density. We have also calculated the *x/3A* line-intensity ratio expected in a recombining plasma, using methods similar to Ref. 4. At electron densities larger than $2 \times 10^{20} \text{ cm}^{-3}$, the *x/3A* ratio becomes independent of the charge-state distribution, owing to large $n=3$ to $n=3$ collisional rates.

In Fig. 3, the calculated *x/3A* Mo^{32+} and Ag^{37+} line-intensity ratios are plotted for temperatures of 300 and 500 eV and they clearly show the density sensitivity of this line-intensity ratio. The figure also indicates this

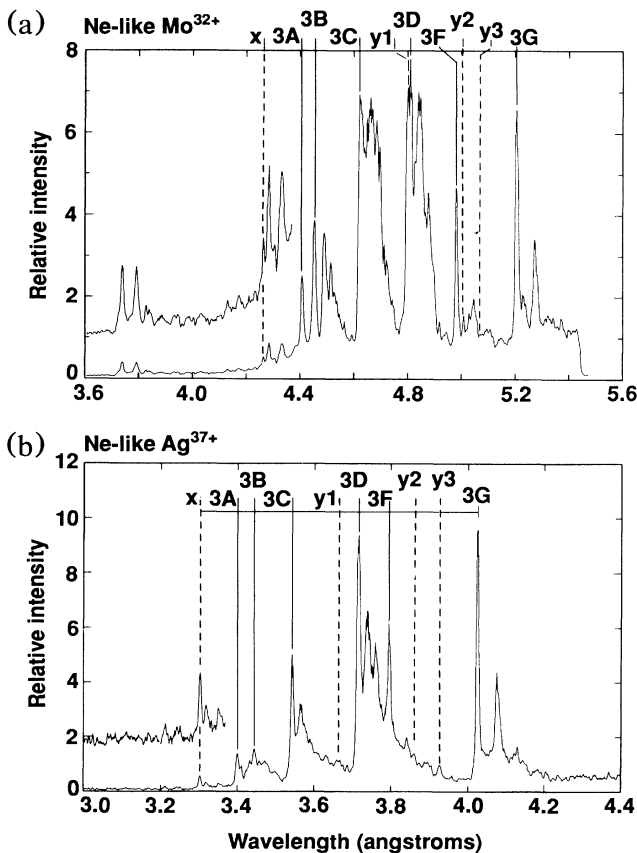


FIG. 2. Densitometer scans for (a) Mo and (b) Ag representing the *L*-shell emission produced by the plasma region 47–94 μm from the target surface for the 230–480-ps time interval. The Ne-like resonance lines are identified using the standard notation (*3G*, . . . , *3A*) of Refs. 3–5. The *x* *E2* line and the predicted locations for the $3p-2p$ *E2* lines, labeled as *y1*, . . . , *y3*, are also indicated.

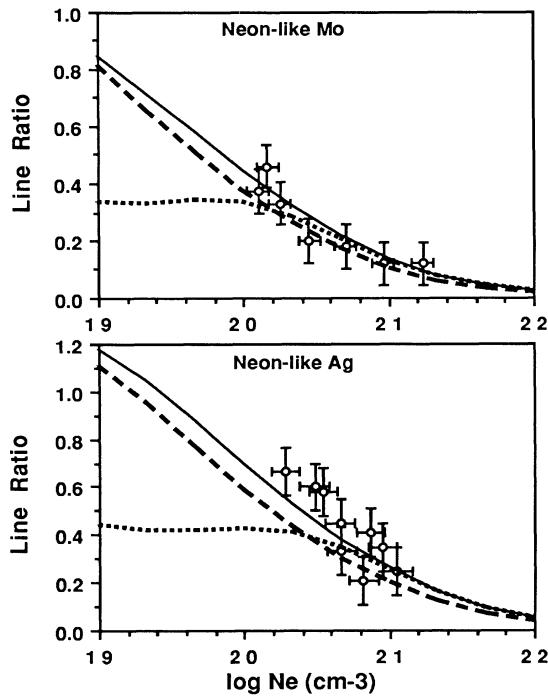


FIG. 3. Experimental $x/3A$ Ne-like line-intensity ratios (open circles) as a function of the electron density measured via laser interferometry for Mo (top) and Ag (bottom), compared to calculated values assuming purely excitation kinetics at 500 eV (solid line) and 300 eV (dashed line) and for recombination kinetics at 500 eV (dotted line).

line ratio is approximately independent of temperature. The measured Mo^{32+} and Ag^{37+} $x/3A$ line-intensity ratios are also plotted in Fig. 3 as a function of the electron density measured at the center of the plasma by holographic interferometry. The vertical error bars represent our estimated $\pm 20\%$ accuracy in the measured line ratio, while the horizontal bars reflect the estimated electron density variation over the 50- μm , 250-ps FCXS space and time intervals. The measured $x/3A$ line ratios are in excellent agreement with the predicted values.

The $E2$ x transition provides a highly attractive density diagnostic. This transition has been observed in laser-produced plasmas for a range of elements and is well isolated from other spectroscopic features. Since the x and $3A$ levels have similar energies, the $x/3A$ line-intensity ratio is insensitive to the electron temperature and to spectral variations in the instrumental response. Furthermore, for densities above $2 \times 10^{20} \text{ cm}^{-3}$, this ratio can be used to diagnose plasmas that are not in charge-state equilibrium. In contrast, the intensities of the $3d-2p$ resonance lines labeled $3F$ and $3G$ are predicted to be highly sensitive to the charge-state distribution and the observed density dependences of these lines do not agree with a model of the neonlike charge state. Thus, ratios using these resonance lines cannot be used reliably without knowledge of the charge-state distribu-

tion.⁴

The observation of the density-dependent $x E2$ line indicates a significant population in the $2s2p^63d(J=2)$ metastable level, which suggests possible population inversions with the resonantly decaying $2s2p^63p(J=1)$ and $2s^22p^53d(J=1)$ levels. The latter inversion is especially significant because the wavelength of the $2p-2s$ transition is below the 44- \AA "water window," at which short-wavelength lasers become useful probes of organic material.¹ We also note that the $3p-2p E2$ lines may be present in the measured neonlike spectra²² (see Fig. 2). The exact identification of these transitions cannot be certain without a comprehensive analysis of the data. These quadrupole line intensities, corrected by the appropriate branching ratio, would provide a direct measurement of the upper-level populations of the $J=2-1$ lasing transitions that have been observed in neonlike lasing schemes.

In summary, we have reported on the measurement of simultaneously space- and time-resolved electric dipole and quadrupole x-ray transitions in Ne-like Mo^{32+} and Ag^{37+} produced in high-power, laser-produced plasmas. We have tested the density dependence of a line-intensity ratio and have found excellent agreement with predictions of a detailed, collisional-radiative model of the Ne-like charge state. At sufficiently high electron densities, this single line-intensity ratio can be used to diagnose plasmas with nonequilibrium charge-state distributions, in contrast with resonance line-intensity ratios previously investigated. These new, spatially and temporally resolved measurements demonstrate the excellent capability now available to probe localized plasmas and directly test available theoretical atomic models.

We gratefully acknowledge the expert technical support of the CHROMA laser staff at KMS Fusion. This work was performed in part under the auspices of the U.S. Department of Energy by LLNL under Contract No. W-7405-Eng-48 and by KMS Fusion under Contract No. DE-AC08-82-DP40152.

¹D. L. Matthews *et al.*, Phys. Rev. Lett. **54**, 110 (1985).

²M. D. Rosen *et al.*, Phys. Rev. Lett. **54**, 106 (1985).

³J. Bailey, R. E. Stewart, J. D. Kilkenny, R. S. Walling, T. W. Phillips, R. J. Fortner, and R. W. Lee, J. Phys. B **19**, 2639 (1986).

⁴W. H. Goldstein, R. S. Walling, J. Bailey, M. H. Chen, R. Fortner, M. Klapisch, T. Phillips, and R. E. Stewart, Phys. Rev. Lett. **58**, 2300 (1987).

⁵R. S. Walling, Ph.D. thesis, University of California, Davis, 1980 (unpublished).

⁶C. J. Cerjan, Phys. Fluids **31**, 3346 (1988).

⁷J.-C. Gauthier, J.-P. Geindre, P. Monier, E. Luc-Koenig, and J.-F. Wyart, J. Phys. B **19**, L385 (1986).

⁸J.-C. Gauthier, P. Monier, J.-F. Wyart, M. Cornille, and J. Dubau, in *Proceedings of the Third International Conference*

on *Radiative Properties of Hot Dense Matter III*, edited by B. Rozsnyai *et al.* (World Scientific, Singapore, 1987), p. 154.

⁹T. W. Phillips and B. J. MacGowan (unpublished data).

¹⁰P. Beiersdorfer *et al.*, Phys. Rev. A **37**, 4153 (1988).

¹¹J. E. Rice *et al.* (to be published).

¹²B. K. F. Young, R. E. Stewart, Gar. E. Busch, C. J. Cerjan, and G. Charatis, Phys. Rev. Lett. **61**, 2851 (1988).

¹³B. K. F. Young, Ph.D. thesis, University of California, Davis, LLNL Report No. UCRL-98692, 1988 (unpublished).

¹⁴B. K. F. Young, G. Charatis, Gar. E. Busch, and R. E. Stewart (to be published).

¹⁵A laser focal spot size of 250 μm was used to overfill the microdot targets. The silver dots were 100 μm in diameter. The Mo-Mg composite targets consisted of a 70- μm dot of alternating layers of Mo and Mg (with an overall thickness of $\geq 1.5 \mu\text{m}$) atop a 170- μm dot of pure Mg (thickness ≥ 1.5

μm).

¹⁶Gar. E. Busch, C. L. Shepard, L. D. Seibert, and J. A. Tarvin, Rev. Sci. Instrum. **56**, 879 (1985).

¹⁷R. W. Lee, B. L. Whitten, and R. E. Strout, II, J. Quant. Spectrosc. Radiat. Transfer **32**, 91 (1983).

¹⁸M. Klapisch, Comput. Phys. Commun. **2**, 239 (1971).

¹⁹M. Klapisch, J. L. Schwob, B. S. Fraenkel, and J. Oreg, J. Opt. Soc. Am. **61**, 148 (1977).

²⁰A. Bar-Shalom, M. Klapisch, and J. Oreg, Phys. Rev. A **38**, 1773 (1988).

²¹K. Reed and A. U. Hazi (private communication).

²²These $2p\text{-}3p$ $E2$ lines were observed in Ref. 7 in laser-produced AgXXXVIII. A calculation of the density dependence of these transitions in six neonlike ions was reported by U. Feldman, J. F. Seely, and A. K. Bhatia, J. Appl. Phys. **58**, 3954 (1985).

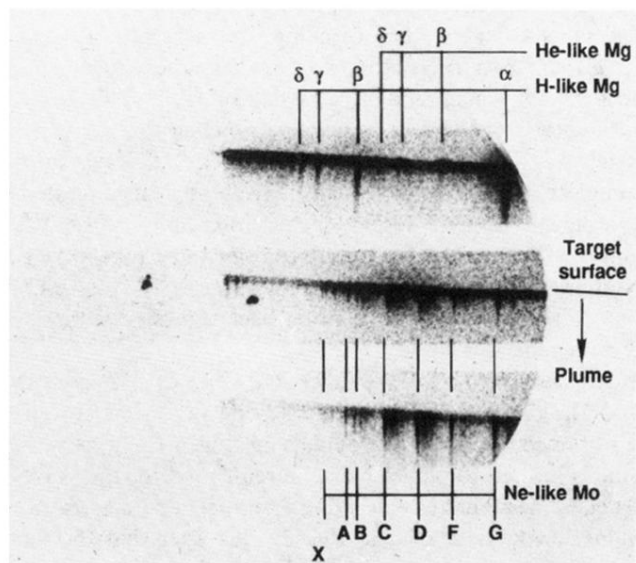


FIG. 1. A set of framed, space-resolved spectra for a Mo-Mg target measured with the FCXS: Mg *K*-shell spectra for 230–480 ps (top), and Mo *L*-shell spectra for 230–480 ps (middle) and 730–980 ps (bottom).